Journal of Power Sources 237 (2013) 128–131

Contents lists available at SciVerse ScienceDirect

Journal of Power Sources

journal homepage: www.elsevier.com/locate/jpowsour

Short communication

The mechanism of sulfur poisoning on the nickel/yttrium-stabilized zirconia anode of solid oxide fuel cells: The role of the oxygen vacancy

Yanxing Zhang [a], Zhansheng Lu [a], Zongxian Yang [a,*], Tom Woo [b]

[a] College of Physics and Electronic Engineering, Henan Normal University, Xinxiang, Henan 453007, PR China
[b] Department of Chemistry, University of Ottawa, K1N 6N5 Canada

HIGHLIGHTS

- The adsorption and diffusion properties of sulfur on the Ni/YSZ are studied.
- Adsorbed sulfur doesn't favor to be located at the stoichiometric Ni/YSZ interface.
- The adsorbed S^- is oxidized to S^{2-} and trapped at the oxygen vacancy.
- The trapped sulfur is very difficult to be removed by the fuel (e.g., H_2).

GRAPHICAL ABSTRACT

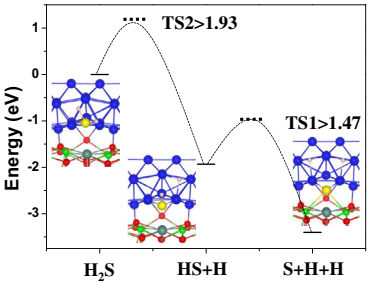

ARTICLE INFO

Article history:
Received 7 December 2012
Received in revised form
5 March 2013
Accepted 8 March 2013
Available online 19 March 2013

Keywords:
Solid oxide fuel cell
Sulfur poisoning
Nickel/yttrium-stabilized zirconia anode
Oxygen vacancy

ABSTRACT

The adsorption and diffusion properties of sulfur on the Ni/YSZ (yttrium-stabilized zirconia) are studied using density functional theory calculations with the particular focus on the influence of the oxygen vacancy at interface. It is found that the adsorbed sulfur does not favor to be located at the stoichiometric Ni/YSZ interface. Instead, it diffuses much easily away from the interface due to the repulsion between the formed S^- and the interface O^{2-}. With the formation of O vacancy at the Ni/YSZ interface, the diffusion direction of sulfur is reversed. The adsorbed S^- diffuses back to the Ni/YSZ interface and is oxidized to S^{2-} and trapped at the oxygen vacancy. Moreover, the trapped sulfur is very difficult to be removed by the fuel (e.g., H_2). The results would further our understanding on the mechanism of sulfur poisoning on the Ni/YSZ anode of solid oxide fuel cells (SOFCs).

1. Introduction

Solid oxide fuel cells (SOFCs) are expected to be a crucial technology in the future of power generation [1,2]. SOFCs offer many desirable advantages compared to other types of fuel cells and conversion devices due to their use of solid electrolytes, lack of moving parts, ability to circumvent precious metal use, high efficiency, low pollution, and fuel flexibility.

The Ni/YSZ (yttrium-stabilized zirconia) is the most popular anode material of SOFCs. However, a major issue in the long-term stability and activity of the anode catalyst is its poor resistance toward poisonous compounds presented in the feed stream. Trace amounts of H_2S presented in biomass generated syngas streams are enough to deactivate the catalyst [3,4]. Therefore, it is desirable to understand the mechanism of sulfur poisoning on the Ni/YSZ anode since such information is applicable to mitigating the deactivation and to developing sulfur tolerant anode material.

Earlier theoretical studies [3,5] showed that sulfur poisoning observed in the low concentration of H_2S at elevated temperature is

* Corresponding author. College of Physics and Electronic Engineering, Henan Normal University, 46 Jianshe Road East, Xinxiang, Henan 453007, PR China. Tel.: +86 373 3329346.
E-mail addresses: yzx@henannu.edu.cn, yzx@htu.cn, zongxian.yang@163.com (Z. Yang).

0378-7753/$ – see front matter © 2013 Elsevier B.V. All rights reserved.
http://dx.doi.org/10.1016/j.jpowsour.2013.03.030

originated from the dissociation of sulfur-containing species and the adsorption of atomic sulfur on the anode surface. The adsorbed H_2S on Ni surfaces has been shown to dissociate above 300 K, with only S remaining on the surface [6]. The strongly adsorbed S species block the active sites on the anode surface and thus increase the resistance to electrochemical oxidation of the fuel. These studies clearly suggest that the elemental sulfur strongly adsorbs on the Ni surfaces with a small activation barrier (E_a) and a large enthalpy (ΔH) (a positive value means that the reaction is exothermic). The adsorbed sulfur blocks the access of hydrogen to the active reaction sites (e.g., the triple-phase boundary, TPB), leading to a large drop in electrochemical activity. The calculations also suggest that the adsorbed sulfur species exist primarily in the form of atomic sulfur instead of molecular species, e.g., H_2S. In fact, the faster or sluggish kinetics is related to the barriers of reactions. The very small E_a means that the barrier for H_2S dissociation is small, but the large exothermic ΔH indicates that the barrier of the reverse reaction of the H_2S dissociation is large. The very small E_a and large exothermic ΔH further imply fast kinetics for sulfur adsorption (as a result of H_2S dissociation) and sluggish kinetics for sulfur removal, which is consistent with the experimental observation of the instant drop in performance upon exposure to H_2S and a very slow recovery in performance after clean hydrogen is switched back. Rasmussen and Hagen [7] also summarized that chemisorption of sulfur on the Ni surface is dominating at relevant testing conditions for SOFCs (700–800 °C and H_2S concentrations below ~50 ppm). More detailed introductions to the sulfur poisoning either experiments or DFT studies are shown in the review articles of Cheng et al. [3] and Offer et al. [8].

To save computation time, the above mentioned theoretical studies usually use the simplified model as H_2S interaction with a metallic anode surface at the double-phase boundary (2PB) (e.g., H_2S–Ni). Generally, the theoretical studies on the sulfur poisoning mechanism [9–13] mostly focus on the 2PB. However, experimental results indicated that sulfur tolerance was in fact improved by using Ni/Sc_2O_3 [14] or Ni/Gd_2O_3 [15]-doped ZrO_2 electrolytes, which suggest at least, that sulfur tolerance depends strongly on anode and electrolyte materials besides nickel itself. To this end, we study the sulfur tolerance properties of Ni/YSZ, in order to clarify the roles of the YSZ or the Ni/YSZ interface played in the sulfur poisoning. More importantly, Shishkin and Ziegler's studies on hydrogen oxidation at the Ni/YSZ interface [16,17] indicated that the most active sites are located at the Ni/YSZ interface. Therefore, the knowledge about the contributions of the electrolyte to sulfur poisoning and the behaviors of the adsorbed sulfur on the active reaction sites (e.g., TPB) and the role of oxygen vacancy at the Ni/YSZ interface (Ni/YSZ–O_v) on the sulfur adsorption is especially important to deeply understand the sulfur poisoning of the anodes of the SOFCs. Furthermore, in experiments, the characterization of sulfur–anode interactions at the TPB appears to be even more challenging given the complexity of the reaction and many species involved (Ni, YSZ, H_2, H_2O, H_2S, and various adsorbed species and lattice defects like oxygen vacancies).

In this work, based on Shishkin and Ziegler's Ni/YSZ model [16], we study the adsorption and diffusion properties of S on the Ni/YSZ interface and the role of interface oxygen vacancy (Ni/YSZ–O_v) on the sulfur adsorption.

2. Model and computation method

All calculations presented in this work are performed employing the periodic density functional theory (DFT) method implemented in the Vienna Ab-Initio Simulation Package (VASP) [18]. The exchange–correlation interactions are treated with the Perdew–Burke–Ernzerhof (PBE) functional [19]. Spin-polarized calculations are applied throughout. The electron–ion interactions are treated using the projector augmented wave (PAW) method [20,21]. The wave functions are expanded in plane waves with a cut off energy of 408 eV. A supercell model as that used in the Shishkin and Ziegler's work [16] is adopted to model the Ni/YSZ cermet, which includes a substrate with the dimensions of 12.56 × 7.25 Å and a vacuum layer of 15 Å in the direction perpendicular to the substrate as shown in Fig. 1. The Monkforst–Pack k-point mesh of 2 × 3 × 1 is used for the Brillouin zone (BZ) sampling. The atoms in the bottom multilayer are kept fixed for all calculations. Structural optimization of all systems is performed until the atomic forces drop below 0.02 eV $Å^{-1}$. The climbing image nudged elastic band method (CI-NEB) [22] method is employed for calculations of transition states and migration barriers. The adsorption energy of a sulfur atom is defined by

$$E_{ads} = E_S + E_{Ni/YSZ\ or\ Ni/YSZ-O_v} - E_{S-Ni/YSZ\ or\ S-Ni/YSZ-O_v} \quad (1)$$

where E_S is the energy of a single S atom simulated in the 8 × 8 × 8 Å box; $E_{S-Ni/YSZ\ or\ S-Ni/YSZ-O_v}$ and $E_{Ni/YSZ\ or\ Ni/YSZ-O_v}$ are the total energies of Ni/YSZ or Ni/YSZ–O_v with and without the S adsorbate, respectively. The $3s^23p^4$ of S, $2s^22p^4$ of O, $3d^84s^2$ of Ni, $4d^25s^2$ of Zr and $4s^24p^65s^24d^1$ of Y are treated as valence electrons in the DFT calculations. The Bader charge [23] analysis scheme is applied to determine the atomic charges and charge transfer. We try to use the international system of units (SI) in this paper. However, we keep some of the popular units used in the micro world and give their equivalent in SI for clarity, e.g., 1 eV = 1.60217733 × 10^{-19} J; 1 Å = 10^{-10} m; 1 e = −1.60217733 × 10^{-19} C and 1 eV $Å^{-1}$ = 1.60217733 × 10^{-9} N.

3. Results and discussions

3.1. The adsorption and diffusion of sulfur on the stoichiometric Ni/YSZ interface

It was indicated that the hydrogen oxidation takes place on the oxygen atoms in the narrow interface between nickel and YSZ as pointed out in Shishkin's work [17], which can be described as (a) a pair of hydrogen atoms adsorbed on the Ni surface, (b) spillover of the first hydrogen to the interface oxygen, (c) migration of the second hydrogen toward the interface oxygen, and (d) hydrogen oxidation with the formation of a water molecule (in the gas phase)

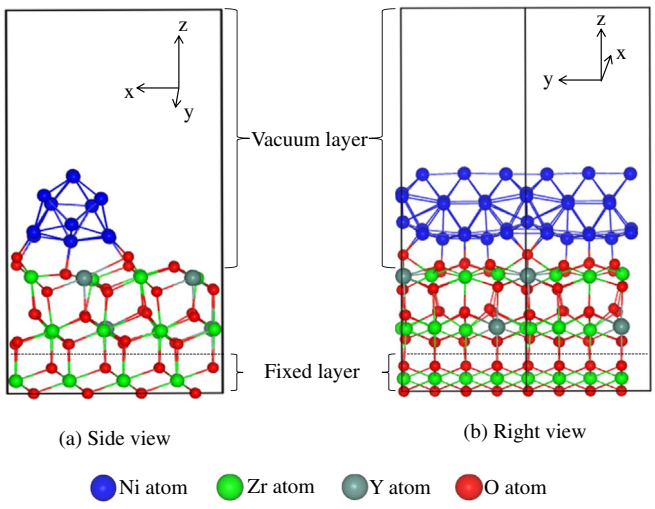

Fig. 1. The model of Ni/YSZ cermet (a) side view (b) right view.

accompanied with an interface oxygen vacancy. Previous predictions for the mechanism of sulfur poisoning on the Ni/YSZ anode are that the adsorbed sulfur blocks the access of hydrogen to the active reaction sites (e.g., TPB), leading to a large drop in electrochemical activity. Therefore, we select four adsorption configurations with S located at the positions marked as I, II, III, and IV as shown in Fig. 2(a). The adsorption properties are summarized in Table 1, which shows that the S adsorption is much more unfavorable and less charged at the interface site I as compared to those at sites II, III, and IV. This might be mainly attributed to the repulsion between the adsorbed S^{-} and the interface O^{2-}. Based on the adsorption configuration with S at site I as depicted in the inset of Fig. 2(b), we can see that upon the adsorption of sulfur, the neighboring interface oxygen sinks by about 0.24 Å into the surface, and the sulfur forms a shorter S–Ni bond with the upper Ni (2.12 Å) as compared with the lower layer Ni (2.21 Å). Based on the Coulomb's law, the S–O repulsion would decay quickly from site I to II, III and IV, in agreement with the variation of their adsorption energies, which increase from 4.60 to 5.30 eV. As a result, the adsorbed S diffuses much easily from site I to II, III and IV, as indicated by the energy profile shown in Fig. 2(b). The diffusion of the adsorbed sulfur atom from site I to II has the smallest barrier of 0.07 eV with a quite big reverse barrier (0.55 eV). The adsorbed sulfur would further experience small barriers of 0.36 (from II to III) and 0.27 eV (from III to IV) and stays at the most favorable adsorption site IV.

3.2. The adsorption and diffusion of sulfur on the Ni/YSZ–O_v interface

From the above results we know that the adsorbed S does not favor the interface site I. Instead it diffuses easily from the interface site to the most favorable site IV on the stoichiometric Ni/YSZ. In other words, the adsorbed S does not block the most active interface site I due to the repulsion between the adsorbed S^{-} and the interface O^{2-}. However, the oxygen vacancy would usually exist after the hydrogen oxidation at the Ni/YSZ interface, as shown in Shishkin's recent work [17]. To this end, the adsorption of sulfur on the interface of Ni/YSZ–O_v is considered. The adsorption properties are summarized in Table 1, from which we can see that the adsorption of sulfur at the Ni/YSZ–O_v interface is enhanced at the corresponding sites as compared with that on the stoichiometric Ni/YSZ interface. The adsorption energy is increased by as much as 0.86 eV at the interface site I, which becomes the most favorable site among the four sites studied. Comparatively, the adsorption energies at sites II, III and IV are slightly enhanced by 0.09, 0.04, and 0.05 eV, respectively. Although there is a significant charge transfer of 0.96 electrons to the supported Ni cluster in the Ni/YSZ–O_v as compared with that in Ni/YSZ, the charges of S adsorbed at the sites I, II, III and IV are hardly changed (e.g., the S atoms at I and III get 0.06, 0.02 *e*, respectively, while those at II and IV keep unchanged). Therefore the adsorption energy enhancement at sites I, II, III and IV could be mainly attributed to the removal of O^{2-}, which leads to the disappearance of the S^{-}–O^{2-} repulsion.

Table 1
The adsorption properties of sulfur on the Ni/YSZ and the Ni/YSZ–O_v. E_{ads}: the adsorption energy of sulfur; $d_{S-Ni(Zr)}$: the bond length of the S–Ni(Zr); S-Chg(e) and Ni-Chg(e): the net charge of the adsorbed sulfur and the nickel cluster, respectively.

	E_{ads} (eV)	d_{S-Ni} (Å)	d_{S-Zr} (Å)	S-Chg (e)	Ni-Chg (e)
Ni/YSZ					−0.12
I	4.60	2.12,2.21,2.20		0.57	−0.60
II	5.08	2.16,2.14,2.15		0.59	−0.68
III	5.22	2.12,2.35,2.30,2.19		0.64	−0.75
IV	5.30	2.18,2.14,2.13		0.62	−0.74
Ni/YSZ–O_v					0.95
O_v	6.21	2.18,2.18	2.63,2.63	1.28	0.02
I	5.46	2.26,2.10,2.11		0.63	0.44
II	5.17	2.17,2.13,2.13		0.59	0.36
III	5.26	2.12,2.33,2.19,2.29		0.66	0.32
IV	5.35	2.12,2.33,2.19,2.29		0.62	0.33

Significantly, the most preferred adsorption site on Ni/YSZ–O_v is the one with the sulfur occupying the interface oxygen vacancy site marked as "O_v", which is equivalent to the substitution of an interface oxygen. The adsorption energy at this site is as large as 6.21 eV and the sulfur gets 1.27 electrons and is reduced to a S^{2-} species, which bonds with two Zr and two Ni cations. From Fig. 3(a) and (b), we can see that with the formation of an interface vacancy, the diffusion direction is reversed. The adsorbed S may easily diffuse back to the Ni/YSZ–O_v interface and occupy the oxygen vacancy. The diffusion from site IV to O_v is almost barrierless (the barrier is as small as 0.03 eV). The escape of the adsorbed sulfur from the O_v site to site II needs to overcome a large barrier of about 1.3 eV, indicating that the adsorbed sulfur is tightly trapped at the O_v site. Thus the oxygen vacancy is poisoned and the oxygen ion transfer would be blocked, which results in the drop of the SOFC performance.

In the TPB of the SOFC, the H_2 in fuel may react with the adsorbed sulfur, which might be one of the possible ways to take the adsorbed sulfur off. However its efficiency is very low. Our test calculations show that the removal of S from the O_v by the reactions (as shown in Fig. 4) of: S + H + H → SH + H → H_2S is

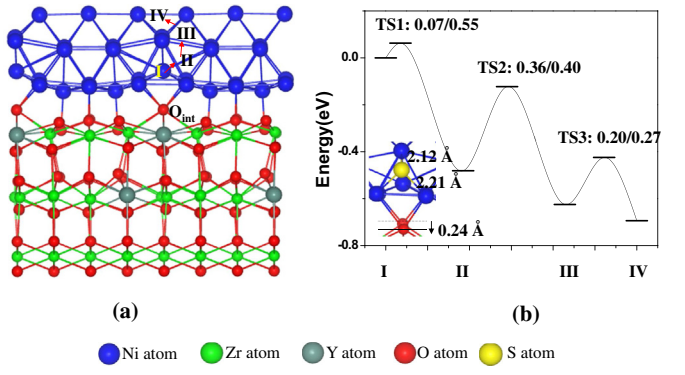

Fig. 2. (a) The adsorption sites of sulfur, and (b) the energy profile for the diffusion of the adsorbed sulfur on the Ni/YSZ. The adsorption configuration at site I is shown as an inset in (b). The two sets of values (such as, TS1: 0.07/0.55) represent the forward/reverse barriers, respectively. The same notations apply for those in Fig. 3.

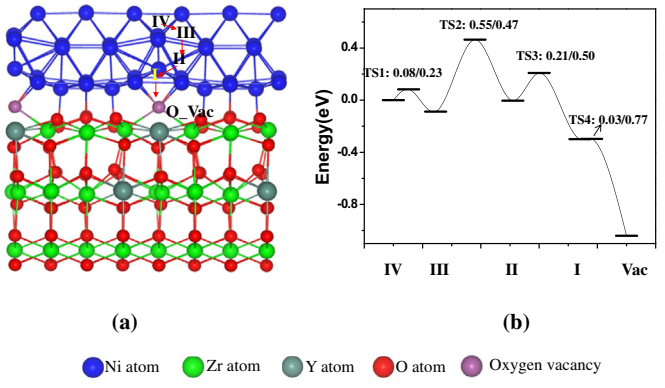

Fig. 3. (a) The adsorption sites of sulfur, and (b) the energy profile for the diffusion of the adsorbed sulfur on Ni/YSZ–O_v. The vacancy (O_v) is shown as a purple ball. (For interpretation of the references to color in this figure legend, the reader is referred to the web version of this article.)

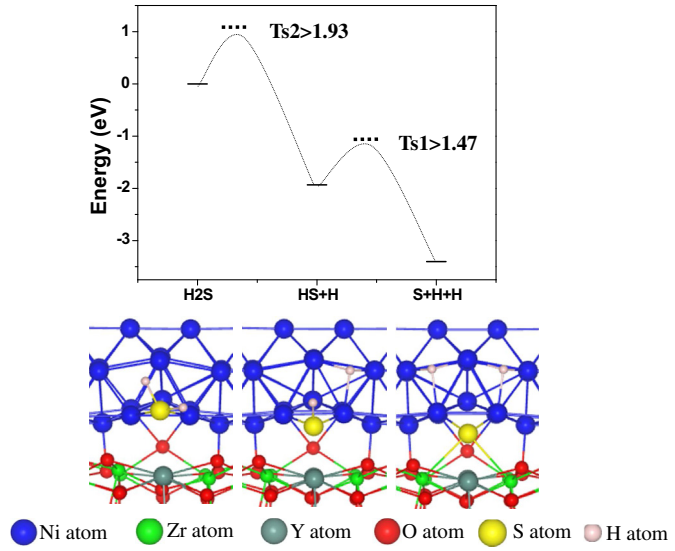

Fig. 4. The energy changes in the reactions of H + S → HS, and HS + H → H_2S at Ni/YSZ–O_v. Since the two elementary dissociation steps (H_2S → HS + H and HS → H + S) of H_2S on the Ni/YSZ–O_v are both exothermic with reaction energies of 1.93 and 1.47 eV, respectively, the barriers for the reverse reactions would be equal to or bigger than the values of 1.93 or 1.47 eV. We do not calculate the barriers in DFT, instead we suppose a value and represent by '…'.

thermodynamically quite unfavorable, since the two elementary dissociation steps (H_2S → HS + H and HS → H + S) of H_2S on the Ni/YSZ–O_v are both exothermic with reaction energies of 1.93 and 1.47 eV, respectively, which are even higher than those on the slab models with the double-phase boundary of Ni(111) [13] (0.98 and 0.86 eV) or Ni(100) [13] (1.56 and 1.05 eV).

4. Conclusion

The *ab initio* density functional theory calculations are performed to study the adsorption and diffusion properties of sulfur on the stoichiometric Ni/YSZ interface and the Ni/YSZ interface with an oxygen vacancy (Ni/YSZ–O_v). It is found that the adsorbed S does not favor to be adsorbed at the stoichiometric Ni/YSZ interface. Instead, it diffuses much easily away from the stoichiometric Ni/YSZ interface due to the repulsion between adsorbed S^- and the interface O^{2-}. However, when an O vacancy is introduced at the Ni/YSZ interface, the diffusion direction is reversed. The adsorbed S diffuses back to the Ni/YSZ–O_v interface and is trapped at the oxygen vacancy, and therefore blocks the pathway of the oxygen ion transfer. As a result, the oxygen ion transfer resistance would be increased and the SOFC performance would drop. Trace amounts of sulfur would block the oxygen vacancy sites at the interface and induce the instant and significant drop in performance of SOFC. The results of this work would further our understanding on the mechanism of sulfur poisoning on the Ni/YSZ anode of SOFC.

Acknowledgments

This work was supported by the National Natural Science Foundation of China (Grant Nos. 11174070 and 11147006) and the Innovation Scientists and Technicians Troop Construction Projects of Henan Province, China (Grant No. 104200510014).

References

[1] R.M. Ormerod, Chem. Soc. Rev. 32 (2003) 17–28.
[2] M.C. Williams, J.P. Strakey, W.A. Surdoval, L.C. Wilson, Solid State Ionics 177 (2006) 2039–2044.
[3] Z. Cheng, J.H. Wang, Y.M. Choi, L. Yang, M. Lin, M. Liu, Energy Environ. Sci. 4 (2011) 4380–4409.
[4] Y. Matsuzaki, I. Yasuda, Solid State Ionics 132 (2000) 261–269.
[5] D.R. Alfonso, Surf. Sci. 602 (2008) 2758–2768.
[6] E. Hardegree, P. Ho, J. White, Surf. Sci. 165 (1986) 488–506.
[7] J.F.B. Rasmussen, A. Hagen, J. Power Sources 191 (2009) 534–541.
[8] G.J. Offer, J. Mermelstein, E. Brightman, N.P. Brandon, J. Am. Ceram. Soc. 92 (2009) 763–780.
[9] D.S. Monder, K. Karan, J. Phys. Chem. C 114 (2010) 22597–22602.
[10] N.M. Galea, E.S. Kadantsev, T. Ziegler, J. Phys. Chem. C 111 (2007) 14457–14468.
[11] N.M. Galea, J.M.H. Lo, T. Ziegler, J. Catal. 263 (2009) 380–389.
[12] J.-H. Wang, M. Liu, J. Power Sources 176 (2008) 23–30.
[13] J.-H. Wang, M. Liu, Electrochem. Commun. 9 (2007) 2212–2217.
[14] K. Sasaki, K. Susuki, A. Iyoshi, M. Uchimura, N. Imamura, H. Kusaba, Y. Teraoka, H. Fuchino, K. Tsujimoto, Y. Uchida, J. Electrochem. Soc. 153 (2006) A2023–A2029.
[15] L.L. Zheng, X. Wang, L. Zhang, J.-Y. Wang, S.P. Jiang, Int. J. Hydrogen Energy 37 (2012) 10299–10310.
[16] M. Shishkin, T. Ziegler, J. Phys. Chem. C 113 (2009) 21667–21678.
[17] M. Shishkin, T. Ziegler, J. Phys. Chem. C 114 (2010) 11209–11214.
[18] G. Kresse, J. Furthmüller, Phys. Rev. B 54 (1996) 11169.
[19] J.P. Perdew, K. Burke, M. Ernzerhof, Phys. Rev. Lett. 77 (1996) 3865–3868.
[20] P.E. Blöchl, Phys. Rev. B 50 (1994) 17953.
[21] G. Kresse, D. Joubert, Phys. Rev. B 59 (1999) 1758.
[22] G. Henkelman, B.P. Uberuaga, H. Jónsson, J. Chem. Phys. 113 (2000) 9901.
[23] G. Henkelman, A. Arnaldsson, H. Jónsson, Comput. Mater. Sci. 36 (2006) 354–360.